Reduction of Acetonitrile by Hydrated Magnesium Cations Mg + (H 2 O) n (n ≈20–60) in the Gas Phase

ARTICLE *in* CHEMPLUSCHEM · SEPTEMBER 2013

Impact Factor: 3 · DOI: 10.1002/cplu.201300170

6 AUTHORS, INCLUDING:

Amou Akhgarnusch
Christian-Albrechts-Universität zu Kiel
8 PUBLICATIONS **17** CITATIONS
SEE PROFILE

Qiang Hao
City University of Hong Kong
25 PUBLICATIONS **128** CITATIONS
SEE PROFILE

Martin Beyer
University of Innsbruck
140 PUBLICATIONS **3,524** CITATIONS
SEE PROFILE

Chi-Kit Siu
City University of Hong Kong
59 PUBLICATIONS **733** CITATIONS
SEE PROFILE

ChemPubSoc Europe

DOI: 10.1002/cplu.201300170

SPECIAL ISSUE

Reduction of Acetonitrile by Hydrated Magnesium Cations $Mg^+(H_2O)_n$ ($n \approx 20$–60) in the Gas Phase

Tim-Wai Lam,[a] Christian van der Linde,[b] Amou Akhgarnusch,[b] Qiang Hao,[a] Martin K. Beyer,*[b] and Chi-Kit Siu*[a]

In memory of Detlef Schröder

Ion–molecule reactions of $Mg^+(H_2O)_n$ ($n \approx 20$–60) with CH_3CN are studied by Fourier-transform ion-cyclotron resonance mass spectrometry. Collision with CH_3CN initiates the formation of $MgOH^+(H_2O)_{n-1}$ together with $CH_3CHN^\bullet$ or $CH_3CNH^\bullet$, which is similar to the reaction of hydrated electrons $(H_2O)_n^-$ with CH_3CN. In subsequent reaction steps, three more CH_3CN molecules are taken up by the clusters, to form $MgOH^+(CH_3CN)_3$ after a reaction delay of 60 seconds. Density functional theory (DFT) calculations at the M06/6-31++G(d,p) level of theory suggest that the bending motion of CH_3CN allows the unpaired electron that is solvated out from the Mg center to localize in a π*(C–N)-like orbital of the bent $CH_3CN^{\bullet-}$, which undergoes spontaneous proton transfer to form $CH_3CNH^\bullet$ or $CH_3CHN^\bullet$, with the former being kinetically more favorable. The reaction energy for a cluster with the hexacoordinated Mg center is more exothermic than that with the pentacoordinated Mg. The $CH_3CNH^\bullet$ or $CH_3CHN^\bullet$ is preferentially solvated on the cluster surface rather than at the first solvation shell of the Mg center. By contrast, the three additional CH_3CN molecules taken up by the resulting $MgOH^+(H_2O)_n$ clusters coordinate directly to the first solvation shell of the $MgOH^+$ core, as revealed by DFT calculations.

Introduction

Singly charged hydrated metal ions in the gas phase have intriguing properties, which have been studied in detail over the last two decades with a fruitful combination of experiment and theory.[1] Exchange experiments with D_2O[2] indicate that hydrated alkali-metal ions[3] as well as most transition-metal ions $M^+(H_2O)_n$, M = Cr, Fe, Co, Ni, Cu, and Zn,[4] consist of a singly charged metal center embedded in a hydrogen-bonded network of intact H_2O molecules, whereas room-temperature black-body infrared radiative dissociation (BIRD)[5] activates an insertion reaction in $Mn^+(H_2O)_n$, which for $n \approx 8$–20 are converted into $HMnOH^+(H_2O)_{n-1}$.[4] In other systems, water activation results in elimination of atomic or molecular hydrogen and oxidation of the metal to the metal hydroxide.[6–14]

Ion–molecule reactions provide insight into the subtle chemistry of these species. Reactions with a strong acid such as HCl induce the elimination of atomic or molecular hydrogen,[10,12,15] and weak acids such as HCOOH also have a promoting effect.[16] Precipitation reactions also work on the single-molecule level in water clusters.[17] Coordination chemistry and charge transfer of hydrated transition-metal ions have been investigated in reactions with O_2, CO_2, and N_2O[18] as well as with NO.[19]

$Mg^+(H_2O)_n$ are certainly among the best-studied singly charged hydrated metal ions in the gas phase.[6,7,9,10,13,14,20,21] These species are only observed for $n < 6$ or $n > 14$, whereas exclusively $MgOH^+(H_2O)_{n-1}$ are present in the mass spectra for $6 \le n \le 14$.[7] Quantum chemical calculations corroborate the interpretation of the experiments[7,9] that for $n > 14$, $Mg^+(H_2O)_n$ consist of a doubly charged magnesium ion and a hydrated electron, with the spin density of the system distributed in a site remote from the metal center.[13,21,22] In a combined experimental and theoretical study, we were able to show that $Mg^+(H_2O)_n$ also exhibit the chemistry of the hydrated electron[23,24] in reactions with O_2 and CO_2, albeit with significantly reduced reaction efficiencies.[22] In the uptake of O_2 or CO_2, the hydrated electron is scavenged by the reactant, and formation of $MgOH^+$ does not occur.

Like O_2 and CO_2, acetonitrile exhibits a specific reactivity toward the hydrated electron. Collisions of $(H_2O)_n^-$ with CH_3CN result in the formation of $OH^-(H_2O)_m$,[25] which are detected by mass spectrometry. Thermochemical arguments require that

[a] T.-W. Lam, Dr. Q. Hao, Prof. Dr. C.-K. Siu
Department of Biology and Chemistry
City University of Hong Kong
83 Tat Chee Avenue, Kowloon Tong, Hong Kong (P. R. China)
Fax: (+852) 3442-0522
E-mail: chiksiu@cityu.edu.hk

[b] Dr. C. van der Linde, A. Akhgarnusch, Prof. Dr. M. K. Beyer
Institut für Physikalische Chemie
Christian-Albrechts-Universität zu Kiel
Olshausenstraße 40, 24098 Kiel (Germany)
Fax: (+49) 431-880-2830
E-mail: beyer@phc.uniso-kiel.de

Supporting information for this article is available on the WWW under http://dx.doi.org/10.1002/cplu.201300170.

$CH_3CHN^{\bullet}$ or $CH_3CNH^{\bullet}$ is formed as the neutral product. The former radical has been observed in ESR studies,[26] the latter was generated by neutralization of protonated acetonitrile.[27] Several experimental studies exist on the solvation and reactions of metal ions with acetonitrile in the gas phase. The interaction of acetonitrile with Nb^+ has been studied by IR multiphoton dissociation spectroscopy,[28] in which reductive nitrile coupling was observed for $Nb^+(CH_3CN)_5$. Solvation of the doubly charged transition-metal ions Co^{2+} and Ni^{2+} with a mixture of acetonitrile and water molecules was studied by photodissociation.[29] Collision-induced dissociation of doubly charged metal ions solvated with acetonitrile $M^{2+}(CH_3CN)_n$ occurs through solvent loss, electron transfer, proton transfer, or heterolytic cleavage of the C–C bond with formation of CH_3^+.[29,30]

To learn more about the chemistry of the hydrated electron in $Mg^+(H_2O)_n$, we investigated the interaction of $Mg^+(H_2O)_n$ ($n \approx 20$–60) with acetonitrile by Fourier-transform ion-cyclotron resonance (FTICR) mass spectrometry and quantum chemical calculations with density functional theory (DFT).

Experimental and Computational Details

The experiments were performed on a modified Bruker/Spectrospin CMS47X FTICR mass spectrometer with a 4.7 T superconducting magnet.[31] $Mg^+(H_2O)_n$ ions were generated in a laser vaporization source and transferred to the ICR cell as described before.[9–11,22] The vaporization laser and frequency doubling crystal were heated by 20 laser shots to avoid changes in the initial cluster distribution, followed by 20 laser shots at 10 Hz and 5 mJ pulse energy to generate the ions. The reaction delay was measured relative to the end of the fill cycle, at nominal $t = 0$ s, so the clusters resided up to 2 seconds in the ICR cell. For this reason, the reaction products were observed at nominal 0 second. Acetonitrile (spectroscopic grade, $\geq$99.9%) was introduced into the ultrahigh-vacuum region through a needle valve at a constant pressure of 8.8×10^{-9} mbar, calibrated with the empirical method of Bartmess et al.[32] using a geometry factor of 3.7.[33] The reaction was monitored by measuring mass spectra at different reaction delays. Collision rates were calculated with the average dipole orientation (ADO)[34] and hard-sphere average dipole orientation (HSA)[35] models for a cluster size of $n = 30$, by using literature values for the dipole moment, polarizability,[36] and viscosity[37] of gaseous acetonitrile.

DFT calculations were performed by using the Gaussian 09 quantum chemical package[38] at the M06/6-31++G(d,p) level of theory, which predicts Mg^+–ligand interaction with a quality comparable to that of high-level ab initio methods.[22] The transition structures were located with one imaginary frequency calculated by the harmonic frequency analyses. Natural population analyses were used for the spin-density calculations. For bulk property calculations, the self-consistent reaction field (SCRF) method with the polarizable-continuum model (PCM) was employed.

Results and Discussion

Ion–molecule reactions

At the end of the trapping period at nominally 0 second reaction delay, $Mg^+(H_2O)_n$ and $MgOH^+(H_2O)_m$ are present in almost

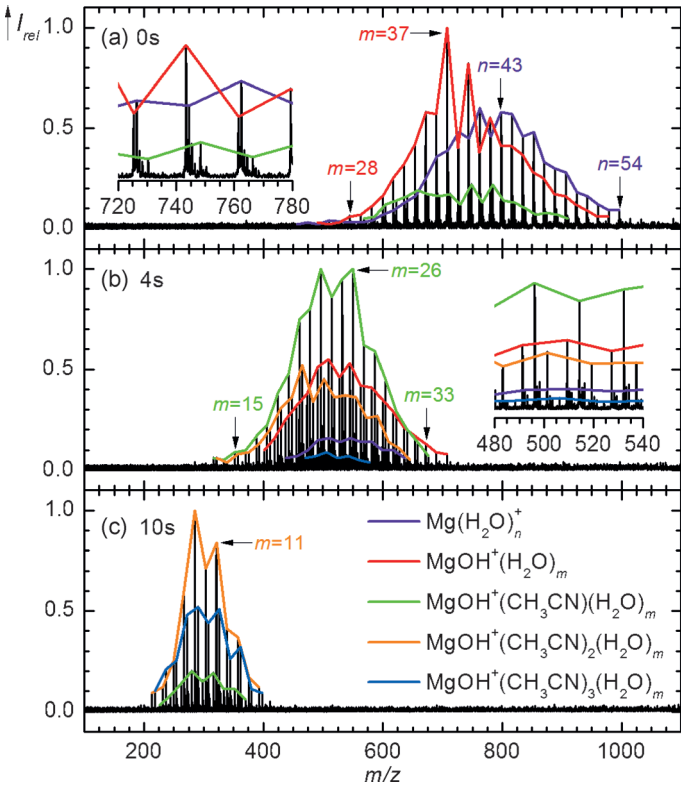

Figure 1. Mass spectra of the reaction of $Mg^+(H_2O)_n$ with acetonitrile after different reaction delays at a pressure of 8.8×10^{-9} mbar. Formation of $Mg(OH)^+(H_2O)_m$ is followed by ligand exchange of up to three acetonitrile molecules.

equal mass spectroscopic intensities (Figure 1a) as well as minor intensities of $MgOH^+(CH_3CN)(H_2O)_m$. The inset in Figure 1a illustrates that data interpretation is made complicated by the isotope pattern of magnesium, with isobaric peaks at $^{24}Mg^+(H_2O)_n$ and $^{25}MgOH^+(H_2O)_{n-1}$. After a delay of 4 seconds (Figure 1b), $Mg^+(H_2O)_n$ have almost disappeared, and $MgOH^+(CH_3CN)(H_2O)_m$ are the dominant species in the mass spectrum. The dominant species at 10 seconds (Figure 1c) are $MgOH^+(CH_3CN)_2(H_2O)_m$, and $MgOH^+(CH_3CN)_3(H_2O)_m$ are also present in high intensities. The only product left after 60 seconds is $MgOH^+(CH_3CN)_3$. The reaction with acetonitrile is accompanied by loss of water molecules owing to BIRD. For $n \leq 21$, blackbody radiation activates formation of atomic hydrogen and $MgOH^+(H_2O)_m$ from $Mg^+(H_2O)_n$ as a parallel reaction.[9,10] Therefore, the cluster size distribution was optimized for large clusters to minimize contributions from this side reaction.

For a quantitative kinetic analysis, the intensity of $^{24}Mg^+(H_2O)_n$ was corrected for the contribution of $^{25}MgOH^+(H_2O)_{n-1}$, based on the intensity of $^{24}MgOH^+(H_2O)_{n-1}$ and the natural isotope abundances of ^{24}Mg and ^{25}Mg, whereas the minor contribution of $^{24}Mg^+(H_2O)_{n-1}(HDO)$ was neglected. The correction is not exact, since the mass difference between $^{24}Mg^+(H_2O)_n$ and $^{25}MgOH^+(H_2O)_{n-1}$ amounts to $\Delta m = 0.00703$ u. However, pressure and lifetime broadening as a result of BIRD make it impossible to resolve the two peaks on our 4.7 T instrument. The kinetics, fitted with a genetic algorithm, nicely exhibits pseudo-

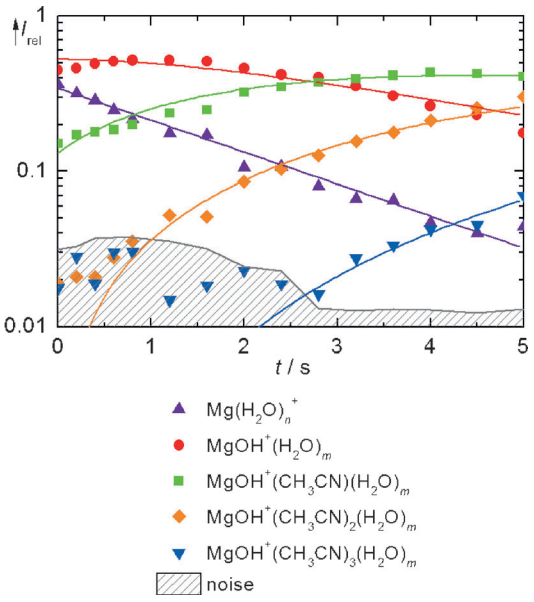

Figure 2. Kinetic fit of the reaction of $Mg^+(H_2O)_n$ with acetonitrile at a pressure of 8.8×10^{-9} mbar for the first 5 seconds. The kinetics shows four consecutive reactions with pseudo-first-order behavior.

first-order behavior for the first 5 seconds of the reaction, as illustrated in Figure 2. In the first reaction step, a hydrogen atom is transferred to acetonitrile, which leads to the formation of hydrated magnesium hydroxide and $CH_3CHN^•$ or $CH_3CNH^•$, written as $[CH_3CN,H]$ [Eq. (1)]:

$$Mg^+(H_2O)_n + CH_3CN \rightarrow MgOH^+(H_2O)_m + [CH_3CN,H] + (n-m)H_2O \quad (1)$$

In subsequent collisions, three molecules of acetonitrile are taken up by the clusters through ligand exchange [Eq. (2)]:

$$MgOH^+(CH_3CN)_{p-1}(H_2O)_n + CH_3CN \rightarrow MgOH^+(CH_3CN)_p(H_2O)_m + (n-m)H_2O \quad p = 1, 2, 3 \quad (2)$$

Table 1 summarizes the absolute rate constants derived from the pseudo-first-order rates and the acetonitrile reactant pressure. In collisions with acetonitrile, $Mg^+(H_2O)_n$ are efficiently converted into $MgOH^+(H_2O)_m$. As shown previously for HCl, O_2, and CO_2,[10,22,23,39] this reflects the reactivity of the hydrated electron $(H_2O)_n^-$, which in collisions with acetonitrile reacts to form $OH^-(H_2O)_m$.[25] In principle, uptake of CH_3CN could also trigger the formation and elimination of a hydrogen atom, but the required selective evaporation of CH_3CN to rationalize the exclusive formation of $MgOH^+(H_2O)_m$ is, in view of the high efficiency of reaction (2), highly improbable. In addition, the zero-point-corrected binding energy of a hydrogen atom to CH_3CN was calculated as 80 kJ mol^{-1} at the G3 level of theory,[40] 103 kJ mol^{-1} at the B3LYP/6-311++G(d,p) level of theory,[41] and 98 kJ mol^{-1} at the M06/6-31++G(d,p) level of theory, with formation of $CH_3CHN^•$ as the energetically most favorable adduct and the global minimum on the $[CH_3CN,H]$ potential energy surface.

Interpretation of the ligand-exchange reaction [Eq. (2)] seems straightforward. Acetonitrile molecules are added until, together with the hydroxide ion, a coordination number of four is reached at the Mg^{2+} center. Spectroscopic studies on Mg^{2+} in bulk CD_3CN, however, report a primary coordination number of six,[42] and a preferential coordination of Mg^{2+} with H_2O in mixtures of water with deuterated acetonitrile, studied for mole fractions of up to 20% H_2O in CD_3CN.[42] But even at the highest water content, the signature of CD_3CN coordinated to Mg^{2+} is strong, thus showing that water does not replace all coordinated acetonitrile molecules in the bulk.[42] If one takes into account that the hydroxide ligand, the internal low temperature of the cluster, and the gas-phase environment have a subtle influence on the coordination chemistry, uptake of three acetonitrile molecules with direct coordination to the Mg^{2+} center is plausible and not in conflict with the bulk spectroscopic result. It is, however, probable that in large clusters, Mg^{2+} is hexacoordinated, with three acetonitrile molecules, one hydroxide ion, and two water molecules.

Magnesium hydroxide formation [Eq. (1)] proceeds, depending on the model, with 64–75% collision rate. The rate constant for reaction (1) is 24 and 115 times higher than the low values observed for uptake of O_2 and CO_2, respectively.[22] This is reasonable, because acetonitrile forms hydrogen bonds, in contrast to O_2 and CO_2, and owing to its large dipole moment it interacts more strongly with the positively charged metal center. The residence time of CH_3CN in the cluster, before a chemical reaction occurs, is therefore significantly longer than for O_2 or CO_2. If the neutral reactant arrives at the cluster surface in a position remote from the reactive site, that is, the hydrated electron, O_2 and CO_2 evaporate quickly, whereas CH_3CN integrates into the hydrogen-bonded network or even coordinates directly to Mg^{2+}. The collision complex has sufficient time to perform the extensive rearrangements, including proton transfer, which are required to form the hydroxide ion and to eliminate the neutral product $[CH_3CN,H]$. Uptake of additional acetonitrile molecules [Eq. (2)] becomes less efficient with increasing number of occupied coordination sites at the Mg^{2+} center.

Table 1. Absolute rate constants k_{abs} [cm^3 s^{-1}] of the reaction of $Mg^+(H_2O)_n$ with CH_3CN. Efficiencies Φ_{ADO} and Φ_{HSA} for collision rates of $k_{ADO}=2.4\times10^{-9}$ and $k_{HSA}=2.8\times10^{-9}$ cm^3 s^{-1} calculated from the ADO and HSA models for $n=30$, respectively.

Reactant	Product	k_{abs} [cm^{-3} s^{-1}]	Φ_{ADO} [%]	Φ_{HSA} [%]
$Mg^+(H_2O)_n$	$MgOH^+(H_2O)_m$	1.8×10^{-9}	75	64
$MgOH^+(H_2O)_m$	$MgOH^+(CH_3CN)(H_2O)_m$	1.5×10^{-9}	63	54
$MgOH^+(CH_3CN)(H_2O)_m$	$MgOH^+(CH_3CN)_2(H_2O)_m$	9.2×10^{-10}	38	33
$MgOH^+(CH_3CN)_2(H_2O)_m$	$MgOH^+(CH_3CN)_3(H_2O)_m$	5.1×10^{-10}	21	18

DFT calculations

Structures and energies of CH_3CN and $CH_3CN^{\bullet-}$

An electron attachment to small gas-phase clusters of CH_3CN can form dipole-bound anions with the excess electron being weakly solvated by the methyl groups of the linear CH_3CN molecules.[43,44] With solvation, the excess electron locates favorably at an orbital with a significant C–N π^* character to form a valence-bound anion, which has a bent geometry with a CCN angle of around 130°.[45] Energies of CH_3CN and $CH_3CN^{\bullet-}$ evaluated at the M06/6-31++G(d,p) level of theory are summarized in Table 2. For CH_3CN, bending the linear CCN bond increases the relative energy to 22 kJ mol^{-1} at 155° and 89 kJ mol^{-1} at 130°. These energies are comparable with those for the molecule being solvated in aqueous solution described by the SCRF method with the PCM. The 6-31++G(d,p) basis set is not adequate to describe the linear dipole-bound state of $CH_3CN^{\bullet-}$, which is incorrectly predicted to be higher-lying than CH_3CN.[43–45] Single-point energy calculations performed with a larger basis set, composed of aug-cc-pVDZ for all atoms and three additional diffuse s and p orbitals for the methyl carbon atom,[44] significantly reduce the relative energy of the dipole-bound $CH_3CN^{\bullet-}$ to −14 kJ mol^{-1}. The basis set effect becomes insignificant for solvated $CH_3CN^{\bullet-}$ because the bent valence-bound geometry is much more favorable with a relative energy of −116 and −121 kJ mol^{-1} as predicted with the 6-31++G(d,p) and the larger basis sets, respectively.

Table 2. Relative energies of CH_3CN and $CH_3CN^{\bullet-}$ with different CCN angles in the gas phase or aqueous solution as described by the polarizable-continuum model (PCM). All geometric parameters (except the constrained angle) are optimized at the M06/6-31++G(d,p) level. Relative energies are obtained at this level. The energies shown in parentheses are single-point energy calculations for the M06/6-31++G(d,p) optimized geometries using aug-cc-pVDZ for all atoms and three additional diffuse functions for the methyl carbon.

		CH_3CN			$CH_3CN^{\bullet-}$		
angle CCN [°]		180	155	130	180	155	130
relative energy [kJ mol^{-1}]	gas phase	0	22	89	66	80	105
		(0)	(22)	(87)	(−14)	(7)	(50)
	solvated (PCM)	0	24	95	−65	−92	−116
		(0)	(23)	(94)	(−72)	(−98)	(−121)

Reactions of hexacoordinated $Mg^+(H_2O)_6$ (6+0) with CH_3CN

Additions of CH_3CN to small six-water model clusters $Mg^+(H_2O)_6$ having the complete hexacoordinated first solvation shell are shown in Figure 3a. The C_3 structure **(6+0)** is −9 kJ mol^{-1} lower-lying than the previously reported C_2 structure,[14] evaluated at the M06/6-31++G(d,p) level. Natural population analysis (NPA) shows that 0.95 of the total spin density is distributed among Mg (0.35) and three water molecules (0.20 each). The CH_3CN addition complex **(6+0)-1** with the CH_3 group pointing to this solvated electron, an analogue of the dipole-bound structure, is 16 kJ mol^{-1} higher than the reactant. Adding CH_3CN to a position remote from the solvated electron to form the lowest-energy complex **(6+0)-2** is exothermic by 66 kJ mol^{-1}. The small $Mg^+(H_2O)_6$ is already fluxional enough to allow facile movements of the solvated electron to various positions, for instance, to produce complexes **(6+0)-3** and **(6+0)-4**. The binding energies of CH_3CN in these solvation structures are around 63–66 kJ mol^{-1}. The relative energies of all these complexes are only slightly changed after the larger basis set with very diffuse functions for the methyl carbon atom[44] is applied, which suggests that the unpaired electron is stabilized by the water cluster rather than the large dipole moment of CH_3CN.

In **(6+0)-2**, CH_3CN is linear. The bond angle tends to decrease if the solvated electron migrates closer to CH_3CN, as in **(6+0)-3**. Further decreasing the bond angle to 157° results in a transition structure **(6+0)-3 TS5** with a relative energy of −45 kJ mol^{-1}. This bending energy of around 18–21 kJ mol^{-1} is comparable with the value predicted for bending a neutral CH_3CN molecule to a similar angle of 155° (22–24 kJ mol^{-1}, Table 2). This indicates that the solvated electron in **(6+0)** does not influence the bending of CH_3CN; instead, it is the bending motion of CH_3CN that provides a π^*(C–N)-like orbital to accommodate some electron density, which is depicted with the spin-density distribution plot for **(6+0)-3 TS5** in Figure 3a. NPA shows that in **(6+0)-3 TS5** there is 0.36 of the total spin density localized in CH_3CN (0.27 at the cyano carbon and 0.05 at the nitrogen). Intrinsic reaction coordinate calculations for **(6+0)-3 TS5** result in the reactant **(6+0)-3** or a spontaneous proton transfer from a water molecule to the nitrogen, to yield the product **(6+0)-5*E***, which is a solvation complex between $MgOH^+(H_2O)_5$ (**$(6+0)_{-H}$**) and the *E* configuration of $CH_3CNH^{\bullet}$ with the spin density mainly located at the cyano carbon (0.81). The relative energy of this *E*-isomer product is −98 kJ mol^{-1}, which is 10 kJ mol^{-1} below the less stable *Z* isomer **(6+0)-5*Z***.

Another transition structure **(6+0)-4 TS6** with a relative energy of −38 kJ mol^{-1} is also located. In this structure, the CH_3CN is also bent (159°) and gives the π^*(C–N)-like orbital to accommodate 0.29 of the total spin density in CH_3CN (0.10 on the cyano carbon and 0.15 on the nitrogen). The relative energy of the product **(6+0)-6** is −119 kJ mol^{-1} and the spin density is almost exclusively located at the nitrogen atom (0.97). The energies of the two transition structures leading, respectively, to $CH_3CNH^{\bullet}$ and $CH_3CHN^{\bullet}$ are comparable, which suggests that formation of these two products is possible with the former being slightly more favorable kinetically. The binding energies of *E*/*Z*-$CH_3CNH^{\bullet}$ and $CH_3CHN^{\bullet}$ to the corresponding cluster are similar, around 56–58 kJ mol^{-1}, which are comparable with the energy required for water evaporation.

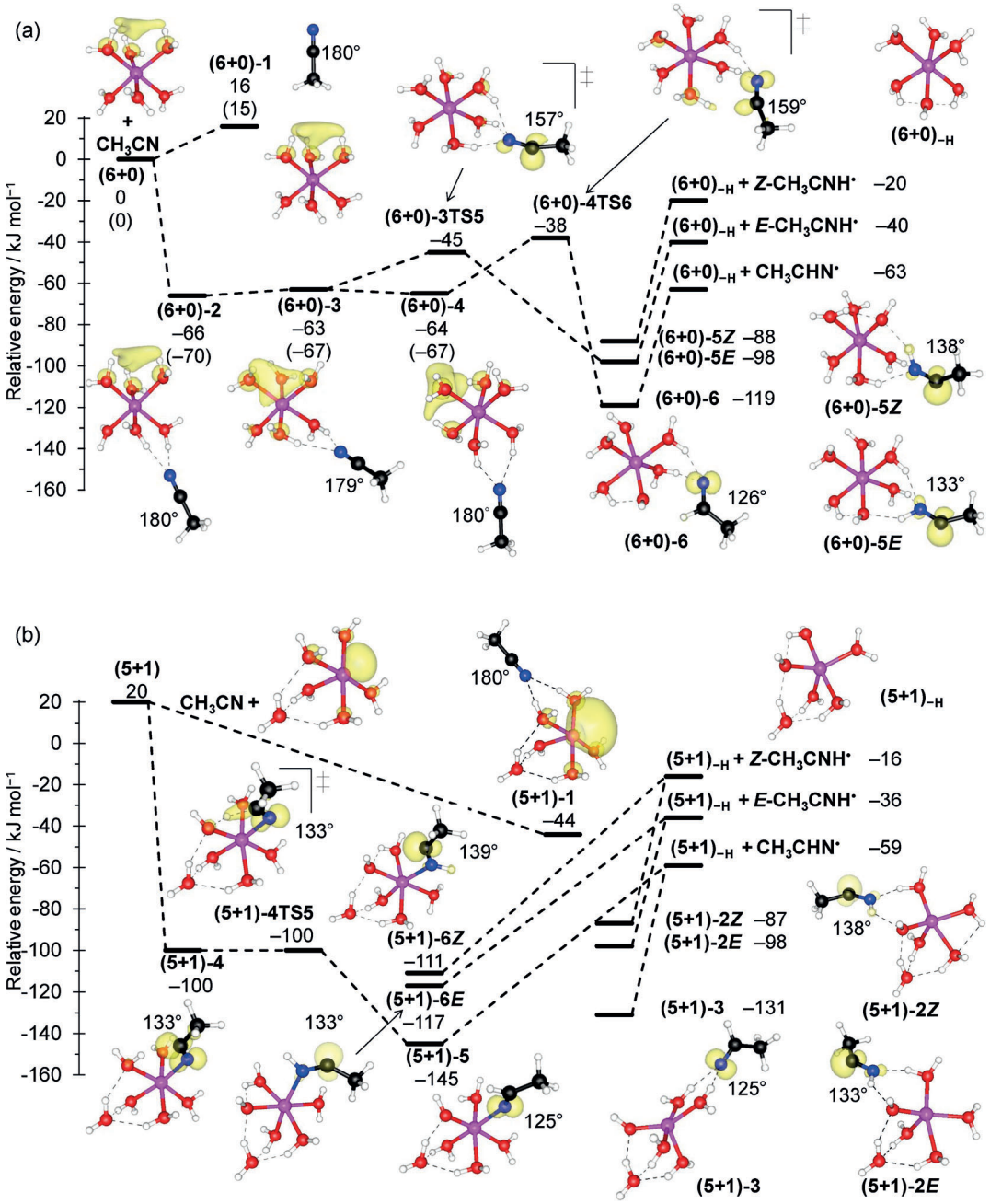

Figure 3. Reaction energy of $Mg^+(H_2O)_6$ with CH_3CN calculated at the M06/6-31++G(d,p) level of theory. Hexa- and pentacoordinated Mg structures ((**6+0**) and (**5+1**), respectively) were considered. Energies in parentheses are calculated with the very large basis set described by Takayanagi.[44] Spin density isosurfaces are shown in yellow.

Reactions of pentacoordinated $Mg^+(H_2O)_6$ (5+1) with CH_3CN

Figure 3b shows the solvation structures for the pentacoordinated $Mg^+(H_2O)_6$ (**5+1**), which is 20 kJ mol^{-1} higher-lying than (**6+0**). The binding energy of CH_3CN onto (**5+1**) giving (**5+1**)-**1** is 64 kJ mol^{-1} (−44 kJ mol^{-1} relative to (**6+0**)), which is comparable with that for (**6+0**). No transition structure associated with the formation of $CH_3CN^{\bullet-}$ can be located. This is probably because in (**5+1**)-**1** the spin density is still mainly located at the Mg center with a value of 0.82, which is significantly larger than that, for instance, in (**6+0**)-**3** of 0.29. The spin density of Mg remains constant (0.80–0.82) during a CCN angle scan calculation for (**5+1**)-**1** from linear down to around 140°, at which still only 0.03 spin density is transferred to CH_3CN. For comparison with the hexacoordinated clusters, the presumable reaction products (**5+1**)-**2*E*** (−98 kJ mol^{-1}), (**5+1**)-**2*Z*** (−87 kJ mol^{-1}), and (**5+1**)-**3** (−131 kJ mol^{-1}) are also located. The binding energies of *E*/*Z*-$CH_3CNH^{\bullet}$ and $CH_3CHN^{\bullet}$ in the corresponding complexes are 62–72 kJ mol^{-1}.

Another, more favorable, addition is with the CH_3CN directly attached to the vacant coordination site of (**5+1**) in the first solvation shell to yield (**5+1**)-**4** with the spin density located at

the cyano carbon (0.38) and the nitrogen (0.45). Product **(5+1)-4** is metastable against proton transfer via the transition structure **(5+1)-4 TS5** with the same relative energy of $-100\ kJ\,mol^{-1}$, to form **(5+1)-5** ($-145\ kJ\,mol^{-1}$), the lowest-energy structure on the potential energy surface for $Mg^+(H_2O)_6 + CH_3CN$ as shown in Figure 3. Similar Mg–N binding structures for *E*/*Z*-$CH_3CNH^\bullet$ are also located as **(5+1)-6(*Z*/*E*)**. These first-shell Mg–N binding energies are around 81–95 $kJ\,mol^{-1}$.

The relative energetics for product formation are quite similar for the **(6+0)** and **(5+1)** pathways, whereas the release of the neutral product requires considerably more energy from the **(5+1)-5** and **(5+1)-6(*Z*/*E*)** intermediates than from their hexacoordinated counterparts.

Reactions of hexa- and pentacoordinated $Mg^+(H_2O)_{16}$ with CH_3CN

The reactions of larger clusters $Mg^+(H_2O)_{16}$[21,22] with CH_3CN, as illustrated in Figure 4, are similar to those of the smaller-cluster analogues. Several surface-solvated structures, similar to the one shown as pathway a in Figure 4, are located with relative energies ranging from -40 to $-48\ kJ\,mol^{-1}$. All products of pathways b–d feature a [CH_3CN,H] radical and a hydroxide ion in the first solvation shell. This suggests that concerted proton transfer[2,46] to form these structures from CH_3CN and $Mg^+(H_2O)_{16}$ faces very small to vanishing barriers. For the hexacoordinated structures, the reaction energies for the formation of $MgOH^+(H_2O)_{15}(L)$ with L = *E*-$CH_3CNH^\bullet$ or $CH_3CHN^\bullet$ (pathway b in Figure 4) are -114 or $-145\ kJ\,mol^{-1}$, respectively, which are of similar magnitudes to that for the formation of the solvent-separated ion pair of $Mg^+(H_2O)_{16}(CO_2)$ ($-129\ kJ\,mol^{-1}$), as evaluated at the same M06/6-31++G(d,p) level of theory.[22]

The reaction energies for the pentacoordinated structures (pathway c in Figure 4) are less exothermic, with a relative energy for L = *E*-$CH_3CNH^\bullet$ and $CH_3CHN^\bullet$ of -79 and $-96\ kJ\,mol^{-1}$, respectively. The hydrated electron in $Mg^+(H_2O)_{16}$ has been completely scavenged by $CH_3CNH^\bullet$ or $CH_3CHN^\bullet$ to give $MgOH^+(H_2O)_{15}$, for which the hexacoordinated geometry becomes thermodynamically more favorable, which would explain the reduced exothermicity for the pentacoordinated structures. Geometry optimizations after L is removed relax to geometries that have relative energies of $-75\ kJ\,mol^{-1}$ (L = *E*-$CH_3CNH^\bullet$) and $-98\ kJ\,mol^{-1}$ (L = $CH_3CHN^\bullet$) for the hexacoordinated $MgOH^+(H_2O)_{15}$ and $-51\ kJ\,mol^{-1}$ (L = *E*-$CH_3CNH^\bullet$) and $-73\ kJ\,mol^{-1}$ (L = $CH_3CHN^\bullet$) for the pentacoordinated $MgOH^+(H_2O)_{15}$. These numbers correspond to binding energies of L of 39–47 $kJ\,mol^{-1}$ for the hexacoordinated clusters and 23–28 $kJ\,mol^{-1}$ for the pentacoordinated clusters.

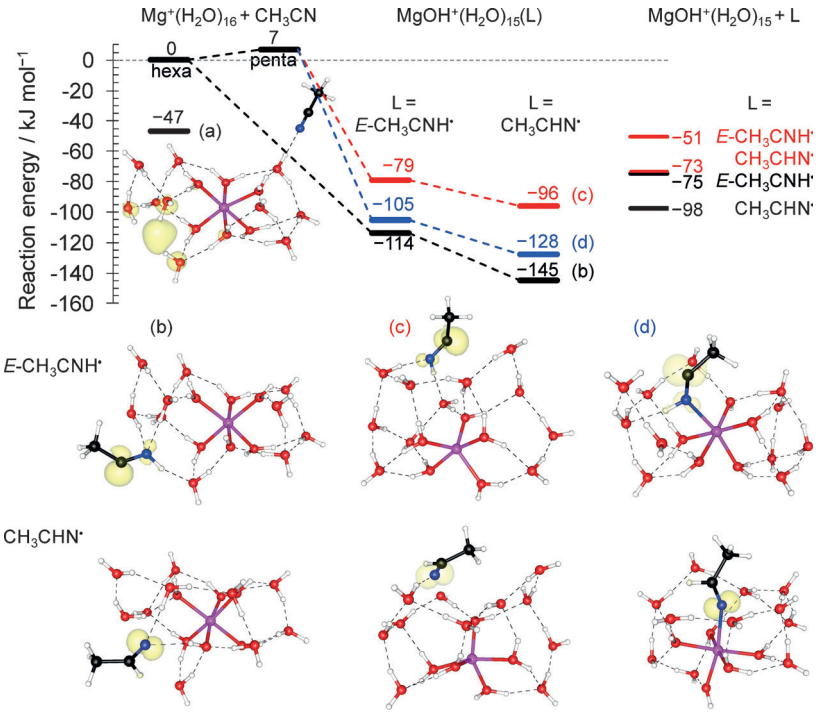

Figure 4. Reaction energy of $Mg^+(H_2O)_{16}$ with CH_3CN calculated at the M06/6-31++G(d,p) level of theory. a) $Mg^+(H_2O)_{16}(CH_3CN)$ (hexacoordinated) with CH_3CN solvated on the surface; b) $MgOH^+(H_2O)_{15}(L)$ (hexacoordinated); c) $MgOH^+(H_2O)_{15}(L)$ (pentacoordinated); d) $MgOH^+(H_2O)_{15}(L)$ (hexacoordinated including L in the first solvation shell). Spin density isosurfaces are shown in yellow.

Binding of *E*-$CH_3CNH^\bullet$ and $CH_3CHN^\bullet$ to the vacant coordination site (pathway d in Figure 4) gives products with relative energies of -105 and $-128\ kJ\,mol^{-1}$, respectively. The Mg···N distances of these *E*-$CH_3CNH^\bullet$ and $CH_3CHN^\bullet$ products are 2.30 and 2.25 Å, respectively, which are longer than the Mg···O distances of around 2.02–2.12 Å.

The present DFT geometry optimizations are certainly not able to describe the fluxional properties of the $Mg^+(H_2O)_{16}$ clusters. Nevertheless, they give an estimated picture for the reaction thermodynamics, which suggests that once $CH_3CNH^\bullet$ or $CH_3CHN^\bullet$ is formed, the resulting Mg^{2+} prefers to be hexacoordinated. Migration of $CH_3CNH^\bullet$ or $CH_3CHN^\bullet$ to the first solvation shell requires a change from the hexacoordinated structures to the pentacoordinated intermediates, which are higher-lying by around 35–49 $kJ\,mol^{-1}$, so that losing the neutral ligands that are initially formed at the cluster surface would be favorable. The reaction predicted theoretically by using the present medium-sized $Mg^+(H_2O)_{16}$ model is aligned with the experimental observations for the larger clusters.

Solvation structures of $MgOH^+(CH_3CN)_p(H_2O)_{5-p}$ (p = 1–5)

To gain insight into the further uptake of CH_3CN by $MgOH^+(H_2O)_n$ through reaction (2), solvent exchange between water at the first solvation shell with acetonitrile was examined by DFT calculations using $MgOH^+(CH_3CN)_p(H_2O)_{5-p}$ ($p = 1–5$) as the model systems [Eq. (3)]:

$$MgOH^+(CH_3CN)_{p-1}(H_2O)_{6-p} + CH_3CN \rightarrow MgOH^+(CH_3CN)_p(H_2O)_{5-p} + H_2O \quad (3)$$

Each model cluster consists of the $MgOH^+$ ion core and five solvent molecules. Hexacoordinated structures for the Mg center were constructed by putting all five solvent molecules together with the hydroxide ion to the first solvation shell of Mg^{2+} **(6+0)$_{-H}$**. Moving one solvent molecule from the first solvation shell to the second results in pentacoordinated structures **(5+1)$_{-H}$**.

Reaction energies of the solvent exchange, reaction (3) for $p = 1–5$, and the lowest-lying structures are shown in Figures 5 and 6, respectively. The solvent-exchange energy increases with the number of acetonitrile molecules added to the first solvation shell of Mg. Regardless of the coordination structures the reaction is exothermic for exchanging up to three acetonitrile molecules ($p = 1–3$), which agrees with the experimental results that only clusters with no more than three acetonitrile molecules were observed. The reaction energies in bulk solution were also calculated by using the SCRF method with the PCM (Figure 5). The reaction energy in bulk solution shows less dependence on the number of acetonitrile molecules, especially for $p = 1–3$ for which the reaction is almost thermoneutral.

The theoretical results suggest that in the large clusters $MgOH^+(H_2O)_n$, a solvated acetonitrile molecule can coordinate to the $MgOH^+$ core by freely exchanging one water molecule from the first solvation shell. After CH_3CN molecules are coordinated directly to the Mg center, the $MgOH^+(CH_3CN)_p$ core is presumably exposed to the cluster surface because of the hydrophobic character of the methyl group. Exchanging the water molecules

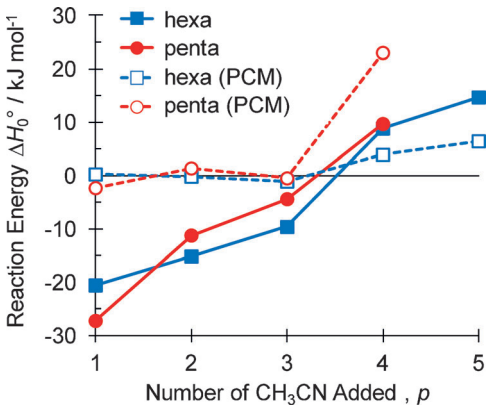

Figure 5. Reaction energies of the solvent exchange [Eq. (3) for $p = 1–5$] at the M06/6-31++G(d,p) level of theory. Results for the gas phase (filled symbols) are compared with calculations in bulk water (open symbols), the latter described by the SCRF method with the PCM.

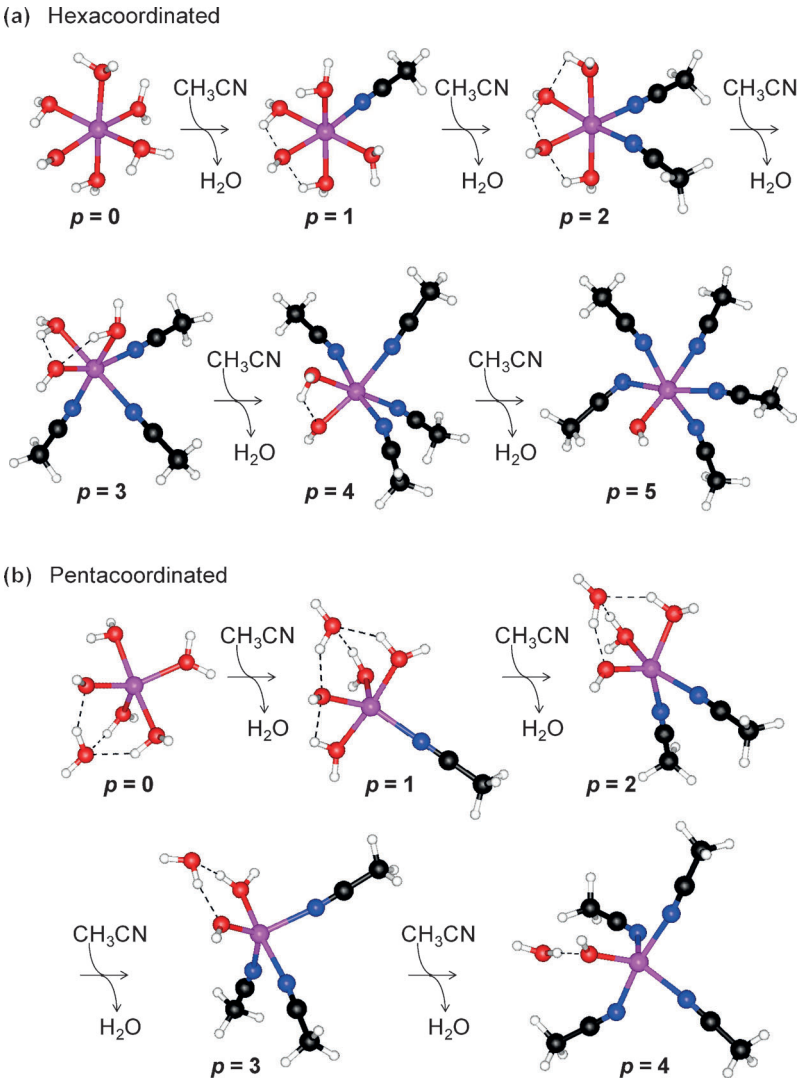

Figure 6. The lowest-lying structures $MgOH^+(CH_3CN)_p(H_2O)_{5-p}$ for the solvent exchange [Eq. (3) for $p = 1–5$] calculated at the M06/6-31++G(d,p) level of theory.

of the first solvation shell of the ionic core with more than three acetonitrile molecules is thermodynamically unfavorable.

Conclusion

The ion–molecule reaction of CH_3CN with $Mg^+(H_2O)_n$ ($n \approx 20$–60) proceeds by a mechanism that is similar to that with a hydrated electron $(H_2O)_n^-$, as revealed by FTICR mass spectrometric experiments and DFT quantum chemical calculations. Collisions of CH_3CN with $Mg^+(H_2O)_n$ initiate the formation of $MgOH^+(H_2O)_{n-1}$ by concomitant loss of $CH_3CHN^\bullet$ or $CH_3CNH^\bullet$. The hydrated electron in $Mg^+(H_2O)_n$ can partially occupy an orbital with π^*(C—N) character in the transition structure, in which CH_3CN is bent with a CCN angle of around 157–159°. This leads to the formation of $CH_3CN^{\bullet-}$, which undergoes spontaneous proton transfer to form $CH_3CNH^\bullet$ or $CH_3CHN^\bullet$, with the former being kinetically more favorable whereas the latter is energetically preferred. The reaction with clusters having a hexacoordinated Mg center is energetically more favorable than that for the pentacoordinated case. The resulting $CH_3CNH^\bullet$ or $CH_3CHN^\bullet$ is preferentially solvated on the cluster surface rather than in the first solvation shell of the Mg center. Up to three additional CH_3CN molecules are taken up by the resulting $MgOH^+(H_2O)_n$, replacing water molecules in the first solvation shell of the $MgOH^+$ core. Compared with the reactions of O_2 and CO_2, CH_3CN reacts much more efficiently with $Mg^+(H_2O)_n$.

Acknowledgements

Financial support from the Deutsche Forschungsgemeinschaft (grant no. BE2505/4-2), DAAD, and PPP Hong Kong (project-ID 50750748) is gratefully acknowledged (M.K.B.). C.-K.S. is grateful for financial support from the Research Grants Council, Hong Kong Special Administrative Region: the General Research Fund, grant number CityU 102911, and the Germany/Hong Kong Joint Research Scheme (grant no. G_HK006/10).

Keywords: density functional calculations · hydrated ions · ion–molecule reactions · mass spectrometry · redox chemistry

[1] a) M. A. Duncan, *Annu. Rev. Phys. Chem.* **1997**, *48*, 69–93; b) K. Fuke, K. Hashimoto, S. Iwata, *Adv. Chem. Phys.* **1999**, *110*, 431–523; c) M. A. Duncan, *Int. J. Mass Spectrom.* **2000**, *200*, 545–569; d) G. Niedner-Schatteburg, V. E. Bondybey, *Chem. Rev.* **2000**, *100*, 4059–4086; e) V. E. Bondybey, M. K. Beyer, *Int. Rev. Phys. Chem.* **2002**, *21*, 277–306; f) M. K. Beyer, *Mass Spectrom. Rev.* **2007**, *26*, 517–541.

[2] Z. Sun, C.-K. Siu, O. P. Balaj, M. Gruber, V. E. Bondybey, M. K. Beyer, *Angew. Chem.* **2006**, *118*, 4133–4135; *Angew. Chem. Int. Ed.* **2006**, *45*, 4027–4030.

[3] V. Vizcaino, B. Puschnigg, S. E. Huber, M. Probst, I. I. Fabrikant, G. A. Gallup, E. Illenberger, P. Scheier, S. Denifl, *New J. Phys.* **2012**, *14*, 043017.

[4] F. Alabarse, J. Haines, O. Cambon, C. Levelut, D. Bourgogne, A. Haidoux, D. Granier, B. Coasne, *Phys. Rev. Lett.* **2012**, *109*, 35701.

[5] a) R. L. Wong, K. Paech, E. R. Williams, *Int. J. Mass Spectrom.* **2004**, *232*, 59–66; b) P. Weis, O. Hampe, S. Gilb, M. M. Kappes, *Chem. Phys. Lett.* **2000**, *321*, 426–432; c) D. Thoelmann, D. S. Tonner, T. B. McMahon, *J. Phys. Chem.* **1994**, *98*, 2002–2004; d) S. M. Stevens, Jr., R. C. Dunbar, W. D. Price, M. Sena, C. H. Watson, L. S. Nichols, J. M. Riveros, D. E. Richardson, J. R. Eyler, *J. Phys. Chem. A* **2004**, *108*, 9892–9900; e) M. Sena, J. M. Riveros, *Rapid Commun. Mass Spectrom.* **1994**, *8*, 1031–1034; f) P. D. Schnier, W. D. Price, R. A. Jockusch, E. R. Williams, *J. Am. Chem. Soc.* **1996**, *118*, 7178–7189; g) T. Schindler, C. Berg, G. Niedner-Schatteburg, V. E. Bondybey, *Chem. Phys. Lett.* **1996**, *250*, 301–308; h) W. D. Price, P. D. Schnier, E. R. Williams, *J. Phys. Chem. B* **1997**, *101*, 664–673; i) A. S. Lemoff, M. F. Bush, E. R. Williams, *J. Am. Chem. Soc.* **2003**, *125*, 13576–13584; j) S. W. Lee, P. Freivogel, T. Schindler, J. L. Beauchamp, *J. Am. Chem. Soc.* **1998**, *120*, 11758–11765; k) O. Hampe, T. Karpuschkin, M. Vonderach, P. Weis, Y. M. Yu, L. B. Gan, W. Klopper, M. M. Kappes, *Phys. Chem. Chem. Phys.* **2011**, *13*, 9818–9823; l) B. S. Fox, M. K. Beyer, V. E. Bondybey, *J. Phys. Chem. A* **2001**, *105*, 6386–6392; m) R. C. Dunbar, T. B. McMahon, *Science* **1998**, *279*, 194–197; n) R. C. Dunbar, *Mass Spectrom. Rev.* **2004**, *23*, 127–158; o) R. C. Dunbar, *J. Phys. Chem.* **1994**, *98*, 8705–8712; p) T. E. Cooper, J. T. O'Brien, E. R. Williams, P. B. Armentrout, *J. Phys. Chem. A* **2010**, *114*, 12646–12655; q) O. P. Balaj, C. B. Berg, S. J. Reitmeier, V. E. Bondybey, M. K. Beyer, *Int. J. Mass Spectrom.* **2009**, *279*, 5–9.

[6] F. Misaizu, M. Sanekata, K. Fuke, S. Iwata, *J. Chem. Phys.* **1994**, *100*, 1161–1170.

[7] M. Sanekata, F. Misaizu, K. Fuke, S. Iwata, K. Hashimoto, *J. Am. Chem. Soc.* **1995**, *117*, 747–754.

[8] a) M. Sanekata, F. Misaizu, K. Fuke, *J. Chem. Phys.* **1996**, *104*, 9768–9778; b) B. M. Reinhard, G. Niedner-Schatteburg, *J. Phys. Chem. A* **2002**, *106*, 7988–7992; c) K. W. Chan, C.-K. Siu, S. Y. Wong, Z.-F. Liu, *J. Chem. Phys.* **2005**, *123*, 124313; d) C. K. Siu, Z. F. Liu, J. S. Tse, *J. Am. Chem. Soc.* **2002**, *124*, 10846–10860; e) B. S. Fox, I. Balteanu, O. P. Balaj, H. C. Liu, M. K. Beyer, V. E. Bondybey, *Phys. Chem. Chem. Phys.* **2002**, *4*, 2224–2228; f) B. Scharfschwerdt, C. van der Linde, O. P. Balaj, I. Herber, D. Schütze, M. K. Beyer, *Low Temp. Phys.* **2012**, *38*, 717–722; g) U. Buck, C. Steinbach, *J. Phys. Chem. A* **1998**, *102*, 7333–7336; h) C. Steinbach, U. Buck, *Phys. Chem. Chem. Phys.* **2005**, *7*, 986–990; i) C. van der Linde, M. K. Beyer, *Phys. Chem. Chem. Phys.* **2011**, *13*, 6776–6778.

[9] C. Berg, U. Achatz, M. Beyer, S. Joos, G. Albert, T. Schindler, G. Niedner-Schatteburg, V. E. Bondybey, *Int. J. Mass Spectrom. Ion Process.* **1997**, *167/168*, 723–734.

[10] C. Berg, M. Beyer, U. Achatz, S. Joos, G. Niedner-Schatteburg, V. E. Bondybey, *Chem. Phys.* **1998**, *239*, 379–392.

[11] M. Beyer, C. Berg, H. W. Görlitzer, T. Schindler, U. Achatz, G. Albert, G. Niedner-Schatteburg, V. E. Bondybey, *J. Am. Chem. Soc.* **1996**, *118*, 7386–7389.

[12] M. Beyer, U. Achatz, C. Berg, S. Joos, G. Niedner-Schatteburg, V. E. Bondybey, *J. Phys. Chem. A* **1999**, *103*, 671–678.

[13] B. M. Reinhard, G. Niedner-Schatteburg, *Phys. Chem. Chem. Phys.* **2002**, *4*, 1471–1477.

[14] C. K. Siu, Z. F. Liu, *Chem. Eur. J.* **2002**, *8*, 3177–3186.

[15] B. S. Fox-Beyer, Z. Sun, I. Balteanu, O. P. Balaj, M. K. Beyer, *Phys. Chem. Chem. Phys.* **2005**, *7*, 981–985.

[16] O. P. Balaj, E. P. F. Lee, I. Balteanu, B. S. Fox, M. K. Beyer, J. M. Dyke, V. E. Bondybey, *Int. J. Mass Spectrom.* **2002**, *220*, 331–341.

[17] a) B. S. Fox, M. K. Beyer, U. Achatz, S. Joos, G. Niedner-Schatteburg, V. E. Bondybey, *J. Phys. Chem. A* **2000**, *104*, 1147–1151; b) B. S. Fox, O. P. Balaj, I. Balteanu, M. K. Beyer, V. E. Bondybey, *J. Am. Chem. Soc.* **2002**, *124*, 172–173; c) B. S. Fox, O. P. Balaj, I. Balteanu, M. K. Beyer, V. E. Bondybey, *Chem. Eur. J.* **2002**, *8*, 5534–5540.

[18] C. van der Linde, S. Hemmann, R. F. Höckendorf, O. P. Balaj, M. K. Beyer, *J. Phys. Chem. A* **2013**, *117*, 1011–1020.

[19] C. van der Linde, R. F. Höckendorf, O. P. Balaj, M. K. Beyer, *Chem. Eur. J.* **2013**, *19*, 3741–3750.

[20] a) N. Okai, H. Ishikawa, K. Fuke, *Chem. Phys. Lett.* **2005**, *415*, 155–160; b) H. Watanabe, S. Iwata, *J. Chem. Phys.* **1998**, *108*, 10078–10083; c) H. Watanabe, S. Iwata, K. Hashimoto, F. Misaizu, K. Fuke, *J. Am. Chem. Soc.* **1995**, *117*, 755–763; d) B. M. Reinhard, A. Lagutschenkov, G. Niedner-Schatteburg, *Phys. Chem. Chem. Phys.* **2004**, *6*, 4268–4275; e) Y. Inokuchi, K. Ohshimo, F. Misaizu, N. Nishi, *Chem. Phys. Lett.* **2004**, *390*, 140–144; f) Y. Inokuchi, K. Ohshimo, F. Misaizu, N. Nishi, *J. Phys. Chem. A* **2004**, *108*, 5034–5040.

[21] C.-K. Siu, Z.-F. Liu, *Phys. Chem. Chem. Phys.* **2005**, *7*, 1005–1013.

[22] C. van der Linde, A. Akhgarnusch, C.-K. Siu, M. K. Beyer, *J. Phys. Chem. A* **2011**, *115*, 10174–10180.

[23] O. P. Balaj, C. K. Siu, I. Balteanu, M. K. Beyer, V. E. Bondybey, *Chem. Eur. J.* **2004**, *10*, 4822–4830.

[24] a) O. P. Balaj, C. K. Siu, L. Balteanu, M. K. Beyer, V. E. Bondybey, *Int. J. Mass Spectrom.* **2004**, *238*, 65 – 74; b) B. C. Garrett, D. A. Dixon, D. M. Camaioni, D. M. Chipman, M. A. Johnson, C. D. Jonah, G. A. Kimmel, J. H. Miller, T. N. Rescigno, P. J. Rossky, S. S. Xantheas, S. D. Colson, A. H. Laufer, D. Ray, P. F. Barbara, D. M. Bartels, K. H. Becker, K. H. Bowen, Jr., S. E. Bradforth, I. Carmichael, J. V. Coe, L. R. Corrales, J. P. Cowin, M. Dupuis, K. B. Eisenthal, J. A. Franz, M. S. Gutowski, K. D. Jordan, B. D. Kay, J. A. LaVerne, S. V. Lymar, T. E. Madey, ·C. W. McCurdy, D. Meisel, S. Mukamel, A. R. Nilsson, T. M. Orlando, N. G. Petrik, S. M. Pimblott, J. R. Rustad, G. K. Schenter, S. J. Singer, A. Tokmakoff, L.-S. Wang, C. Wittig, T. S. Zwier, *Chem. Rev.* **2005**, *105*, 355 – 389; c) R. M. Young, D. M. Neumark, *Chem. Rev.* **2012**, *112*, 5553 – 5577.
[25] O. P. Balaj, I. Balteanu, B. S. Fox-Beyer, M. K. Beyer, V. E. Bondybey, *Angew. Chem.* **2003**, *115*, 5675 – 5677; *Angew. Chem. Int. Ed.* **2003**, *42*, 5516 – 5518.
[26] P. Svejda, D. H. Volman, *J. Phys. Chem.* **1970**, *74*, 1872 – 1875.
[27] X. H. Chen, E. A. Syrstad, F. Turecek, *J. Phys. Chem. A* **2004**, *108*, 4163 – 4173.
[28] B. M. Reinhard, A. Lagutschenkov, J. Lemaire, P. Maitre, P. Boissel, G. Niedner-Schatteburg, *J. Phys. Chem. A* **2004**, *108*, 3350 – 3355.
[29] M. Perera, P. Ganssle, R. B. Metz, *Phys. Chem. Chem. Phys.* **2011**, *13*, 18347 – 18354.
[30] a) M. Kohler, J. A. Leary, *Int. J. Mass Spectrom. Ion Process.* **1997**, *162*, 17 – 34; b) M. Kohler, J. A. Leary, *J. Am. Soc. Mass Spectrom.* **1997**, *8*, 1124 – 1133; c) C. Seto, J. A. Stone, *Int. J. Mass Spectrom. Ion Processes* **1998**, *175*, 263 – 276; d) A. A. Shvartsburg, J. G. Wilkes, J. O. Lay, K. W. Siu, *Chem. Phys. Lett.* **2001**, *350*, 216 – 224; e) N. R. Walker, M. P. Dobson, R. R. Wright, P. E. Barran, J. N. Murrell, A. J. Stace, *J. Am. Chem. Soc.* **2000**, *122*, 11138 – 11145; f) N. R. Walker, R. R. Wright, P. E. Barran, J. N. Murrell, A. J. Stace, *J. Am. Chem. Soc.* **2001**, *123*, 4223 – 4227; g) N. R. Walker, R. R. Wright, A. J. Stace, *J. Am. Chem. Soc.* **1999**, *121*, 4837 – 4844; h) N. R. Walker, R. R. Wright, A. J. Stace, C. A. Woodward, *Int. J. Mass Spectrom.* **1999**, *188*, 113 – 119; i) R. R. Wright, N. R. Walker, S. Firth, A. J. Stace, *J. Phys. Chem. A* **2001**, *105*, 54 – 64; j) C. Y. Xiao, K. Walker, F. Hagelberg, A. El-Nahas, *Int. J. Mass Spectrom.* **2004**, *233*, 87 – 98.
[31] a) M. Allemann, H. Kellerhals, K. P. Wanczek, *Int. J. Mass Spectrom. Ion Phys.* **1983**, *46*, 139 – 142; b) P. Kofel, M. Allemann, H. Kellerhals, K. P. Wanczek, *Int. J. Mass Spectrom. Ion Processes* **1986**, *72*, 53 – 61; c) C. Berg, T. Schindler, G. Niedner-Schatteburg, V. E. Bondybey, *J. Chem. Phys.* **1995**, *102*, 4870 – 4884; d) R. F. Höckendorf, O. P. Balaj, C. van der Linde, M. K. Beyer, *Phys. Chem. Chem. Phys.* **2010**, *12*, 3772 – 3779.
[32] J. E. Bartmess, R. M. Georgiadis, *Vacuum* **1983**, *33*, 149 – 153.
[33] a) T. Schindler, C. Berg, G. Niedner-Schatteburg, V. E. Bondybey, *Ber. Bunsen-Ges.* **1992**, *96*, 1114 – 1120; b) C. van der Linde, R. F. Höckendorf, O. P. Balaj, M. K. Beyer, *Low Temp. Phys.* **2010**, *36*, 411 – 416; c) R. F. Höckendorf, C. van der Linde, O. P. Balaj, I. Herber, M. K. Beyer, *Int. J. Mass Spectrom.* **2011**, *300*, 44 – 49.
[34] a) T. Su, M. T. Bowers, *J. Am. Chem. Soc.* **1973**, *95*, 7609 – 7610; b) T. Su, M. T. Bowers, *Int. J. Mass Spectrom. Ion Processes* **1975**, *17*, 309 – 319.
[35] G. Kummerlöwe, M. K. Beyer, *Int. J. Mass Spectrom.* **2005**, *244*, 84 – 90.
[36] D. R. Lide, *CRC Handbook of Chemistry and Physics*, CRC Press, Boca Raton, **1995**.
[37] *VDI-Wärmeatlas*, Springer, Heidelberg, **2006**.
[38] M. J. Frisch, et al., Gaussian 09, Revision B.01, Gaussian, Inc., Wallingford CT, **2010**. See the Supporting Information for full citation.
[39] C. K. Siu, O. P. Balaj, V. E. Bondybey, M. K. Beyer, *J. Am. Chem. Soc.* **2007**, *129*, 3238 – 3246.
[40] B. S. Wang, H. Hou, Y. S. Gu, *J. Phys. Chem. A* **2001**, *105*, 156 – 164.
[41] X. Zhou, X. Cheng, Y. Zhao, X. Tao, *J. Mol. Struc. THEOCHEM* **2006**, *763*, 123 – 132.
[42] J.-N. Cha, B.-S. Cheong, H.-G. Cho, *J. Phys. Chem. A* **2001**, *105*, 1789 – 1796.
[43] M. Gutowski, K. D. Jordan, P. Skurski, *J. Phys. Chem. A* **1998**, *102*, 2624 – 2633.
[44] T. Takayanagi, *J. Chem. Phys.* **2005**, *122*, 244307.
[45] Q. K. Timerghazin, G. H. Peslherbe, *J. Phys. Chem. B* **2008**, *112*, 520 – 528.
[46] K. Hashimoto, S. Ugajin, S. Yoshida, R. Tazawa, A. Sato, *Chem. Phys.*, **2013**, *419*, 124 – 130.

Received: April 30, 2013
Published online on July 2, 2013

This paper is part of a Special Issue dedicated to the memory of Detlef Schröder. To view the complete issue, visit: http://onlinelibrary.wiley.com/doi/10.1002/cplu.v78.9/issuetoc